The Nature of NO_x Species on BaO(100): An Ab Initio Molecular Dynamics Study

Peter Broqvist,[†] Itai Panas,[‡] and Henrik Grönbeck*,[†]

Department of Applied Physics and Competence Centre for Catalysis and Department of Environmental Inorganic Chemistry, Chalmers University of Technology, SE-412 96 Göteborg, Sweden

Received: June 13, 2005

The dynamics of NO_x species adsorbed on BaO(100) have been investigated with ab initio molecular dynamics simulations at a temperature of 300 °C. Nitrites are found to continuously interconvert between different adsorption configurations. For both nitrites and nitrates, diffusion events between anion sites are observed. These findings support the use of spillover mechanisms often postulated in mechanistic models of catalysts based on the NO_x storage and reduction concept. The large number of possible adsorption configurations are reflected in broad calculated vibrational signatures. These results explain the corresponding property observed in experimental infrared measurements of NO_x species on BaO. The dynamic response of the BaO(100) surface is found to strongly depend on the nature of the surface−adsorbate interaction. The largest distortions are predicted for nitrite adsorption.

I. Introduction

Understanding the interaction between adsorbates and metal oxide surfaces is of fundamental interest in several technological fields where applied heterogeneous catalysis is one example. In heterogeneous catalysis, metal oxides are used for various purposes, such as supports, promoters, and storage materials.[1] Recently, the chemical properties of alkaline earth metal oxides have received considerable attention.[2] The interest originates mainly from the use of BaO in NO_x storage and reduction (NSR) catalysts, which are employed to reduce NO_x emissions from engines working at lean (oxygen excess) conditions.[3−5] The NSR concept is built upon a periodic lean/rich operation of the engine, and the catalyst components are noble metals (platinum and rhodium) together with BaO dispersed on Al_2O_3. NO_x is stored on the BaO component under lean conditions and, subsequently, released and reduced to N_2 during short fuel-rich pulses. At lean operation, it is generally believed that NO_x storage is preceded by NO oxidation over platinum sites. NO_2 is thereafter spilling over to the metal oxide where it is stored. Engine emissions in the form of NO_2 are directly stored on BaO. On the basis of flow reactor experiments and in situ molecular vibrational measurements, surface $Ba(NO_3)_2$ has been suggested as the final storage configuration.[6,7] However, the elementary reaction steps yielding this configuration are to a large degree unknown.

Theoretically, the NO_x storage mechanism has been investigated by exploring adsorption configurations of NO_x species on BaO surfaces and clusters.[8−12] In ref 8, different scenarios were investigated for NO_2 adsorption on a BaO(100) terrace using the density functional theory (DFT) and a slab description of the surface. Nitrites formed upon single NO_2 adsorption. Subsequent adsorption of NO_2 was discovered to form NO_2−Ba−$O_s$$NO_2$ or NO_3−Ba−O_sNO (O_s being a surface oxygen) pairs with high adsorption energies when compared to the energy calculated for single nitrites. The enhanced pair stability was rationalized by electron pairing, mediated by the oxide surface. With this mechanism, it is not surprising that the enhanced stability of nitrite/nitrate pairs later was demonstrated for MgO[13] and $(BaO)_9$ clusters.[9] In addition to energetic and structural characterization of adsorbed NO_x species, vibrational properties were calculated in ref 9 and compared with Fourier transform infrared (FTIR) spectroscopy measurements. In ref 10, NO_2 and NO_3 adsorption on the series of alkaline earth metal oxides (MgO−BaO) were studied using the DFT and an embedded cluster representing the (100) terrace. The substrate basicity was found to determine the adsorbate interaction strength, and the highest binding energies were calculated for BaO. A similar conclusion was presented in ref 11 on the basis of periodic slab calculations for NO_x adsorption on the series of alkaline earth metal oxides. The adsorption of NO_2 on the BaO(100) terraces was recently compared with the adsorption on step and corner sites using the DFT and an embedded cluster description of the BaO.[12] The adsorption energy on step and corner sites was calculated to be higher than that on the terrace.

Sometimes, there is a tendency to exaggerate the importance of specific adsorption configurations because they are easy to characterize theoretically and/or experimentally. In the present paper, we probe a larger part of configuration space by performing ab initio molecular dynamics (AIMD) simulations of nitrites and two nitrite/nitrate pair configurations on BaO-(100). Experimentally, in situ FTIR measurements have revealed broad vibrational bands upon NO_x adsorption on BaO.[6,9,14] This is indicative of species occupying different structural conformations on the time scale of the experiments. Furthermore, investigating the mobility of nitrites and nitrates over BaO is critical, as spillover steps of NO_2 from Pt to BaO generally are postulated in mechanistic models of NO_x storage.[5] For example, such steps had to be assumed in microkinetic models of the NO_x storage on $Pt/BaO/Al_2O_3$ catalysts to fit experimental data.[7]

For alkaline earth metal surfaces, AIMD has previously been used to investigate H_2O adsorption and hydrolysis on MgO surfaces[15,16] and NH_3[17] adsorption on MgO(100). Because both H_2O and NH_3 are physisorbed on MgO(100), these systems are different in nature as compared to NO_x on BaO(100). The

* Corresponding author. E-mail: ghj@fy.chalmers.se.
[†] Department of Applied Physics and Competence Centre for Catalysis.
[‡] Department of Environmental Inorganic Chemistry.

10.1021/jp053178m CCC: $30.25
Published on Web 07/21/2005

adsorbates explored herein are either ionically or covalently bonded to the surface. The present study is, therefore, of general interest, as it addresses the dynamical response of oxide surfaces upon electron abstraction.

II. Computational Method

The simulations were performed within the pseudopotential plane-wave (PP−PW) implementation of the density functional theory (DFT). In particular, the CPMD code was used.[18−21] In previous reports, we have investigated the performance of different exchange-correlation functionals on structural and energetic properties of clean alkaline earth metal oxide surfaces[22] and transition metal adhesion onto such surfaces.[23] These studies show that different approximations to the exchange-correlation functional provide consistent chemical pictures and that the gradient-corrected approximation of the exchange-correlation functional according to Perdew, Burke, and Ernzerhof (PBE)[24] is a reasonable choice when compared to available experimental data. As PBE performs satisfactorily also for the relevant adsorbates,[9] this functional was adapted in the present study.

Norm-conserving angular-dependent pseudopotentials were used to describe the interaction between the valence electrons and the atomic cores.[25] The potentials were derived from solutions to the all-electron (in the case of Ba relativistic) Kohn−Sham equation. To be consistent with the exchange-correlation functional used in the calculations, the potentials were generated with the PBE functional. For barium (generated for Ba^{2+}) the 4s, 4p, and 5d core radii were 0.79, 0.79, and 1.32 Å, respectively. The inclusion of the 5d component is decisive, as 5d states are known to contribute to the bonding in BaO.[26] For oxygen and nitrogen the s and p core radii were 0.69 Å and 0.63 Å, respectively. In the calculations, the one-electron orbitals were expanded in plane waves up to a kinetic energy of 62 Ry. This cutoff energy was sufficient to converge relative energies and molecular structures.[27]

The BaO(100) surface was cleaved from the theoretical bulk lattice and modeled with a p(3 × 3) slab consisting of three layers. Thus, the surface model included 54 atoms (see, e.g., Figure 4a). Repeated slabs were separated by a vacuum width of 12 Å normal to the surface.[28] To describe the situation of a BaO surface terminated from a bulk crystal, the bottommost layer was constrained at bulk distance throughout the calculations. As the employed supercell is sufficiently large, the *k*-point sampling was restricted to the Γ point. The adequateness of this sampling is demonstrated by the structural and energetic results for the clean BaO(100) surface. Calculations of the gas-phase nitrites (NO_2^-) and nitrates (NO_3^-) were done in a cubic (13.2 Å) embedding geometry without periodic images.[29]

Molecular dynamics were performed using the Car−Parrinello method,[18] and a velocity Verlet integrator was used to integrate the equations of motion. A short time step of 5 au (0.12 fs) was used, and the fictitious electron mass was set to 500 au. The molecular dynamics simulations were performed at 300 °C, applying a Nosé−Hoover thermostat. The thermostat frequency was set to 400 cm^{-1}, which is low enough to avoid coupling to the N−O stretching modes. The vibrational signatures of the studied systems were calculated by taking the Fourier transform of the appropriate velocity−velocity autocorrelation function.

In the calculations, the lowest possible multiplet was investigated. Consequently, single NO_2 radicals were investigated in the doublet state and pair configurations in the singlet state. Simulations of four NO_2 radicals on the BaO(100) surface were performed in the singlet state. This is probably a minor approximation, as roughly four electrons are transferred from the surface O(2p) band to the radicals, forming nitrites. In this case, the surface has an even number of electrons that pair up.

The computational approach was tested on BaO in the bulk phase and the NO_2 molecule. In the calculations of the bulk, a unit cell consisting of 64 atoms was employed. The lattice parameter was calculated to 5.59 Å, the cohesive energy to 9.8 eV, and the bulk modulus to 0.64 Mbar. This compares well with previously reported results (5.59 Å, 9.5 eV, 0.68 Mbar),[22] as well as the corresponding experimental values of 5.53 Å,[30] 10.1 eV,[31] and 0.74 Mbar,[30] respectively. Moreover, the bond lengths and bond angle of the NO_2 radical compare favorably with experimental data:[32] 1.21 Å and 134° compared to 1.20 Å and 134°, respectively.

III. Results and Discussion

To put the results from the molecular dynamics simulations in context, static calculations were performed for the clean surface and possible NO_x configurations on BaO(100). These calculations were done at low coverage so as to make clear connections with previously reported data. In this section, the static results are presented first, followed by results from the simulations.

A. Characterization of BaO(100) and NO_x Adsorption Configurations. Surface distortions of metal oxide surfaces are commonly separated into relaxation (ρ) and rumpling (ϵ). Relaxation refers to the interplane distortion, whereas rumpling measures the difference in anion and cation displacement:

$$\rho = \frac{d_a + d_c - 2d_b}{2d_b} \tag{1}$$

$$\epsilon = \frac{d_a - d_c}{d_b} \tag{2}$$

d_a and d_c are the interlayer distance for the anion and the cation, respectively. d_b is the Ba−O nearest neighbor distance in the bulk. For the clean surface, ρ and ϵ are calculated to −3.6% and −3.0%, respectively. These results are consistent with previous results for a four-layer slab (−4.0% and −1.6%).[22] Also, the surface energy of 0.4 J/m^2 agrees with the previous result of 0.4 J/m^2.[22] BaO(100) has not been experimentally characterized with respect to structural and energetic properties.

Different adsorption configurations of NO_2 have been considered, of which three are reported in Figure 1.[33] Two of the structures correspond to "N-down" structures, with a short (a) and long (b) O_s-NO_2 distance, respectively. The third structure, (c), is a bridge geometry with the two oxygen atoms coordinated toward cation barium sites. The three configurations have similar adsorption energies: 1.3 eV (a), 1.3 eV (b), and 1.2 eV (c). Analysis of the spin densities (reported in Figure 1) reveals that NO_2 in (b) and (c) are adsorbed as nitrites. In each of these cases, the spin density on the adsorbate is close to zero, and an electron hole has been created among the surface anions. The assignment of (b) and (c) as nitrites is also consistent with the O−N−O angle being 116°, which is equal to the calculated angle for the nitrite in the gas phase. The interaction between the nitrites and the oxide surface is of an electrostatic nature. For structure (a), the calculated induced dipole moment is 5.0 D. As already pointed out in ref 12, the similarity in adsorption energy for geometries (b) and (c) is indicative of a bond without strong directional character. For structure (a), the spin density is localized on the adsorbate and the surface anion, and the species can be described as a NO_3^{2-} unit. Consequently, although structures (a) and (b) are N-down configurations with

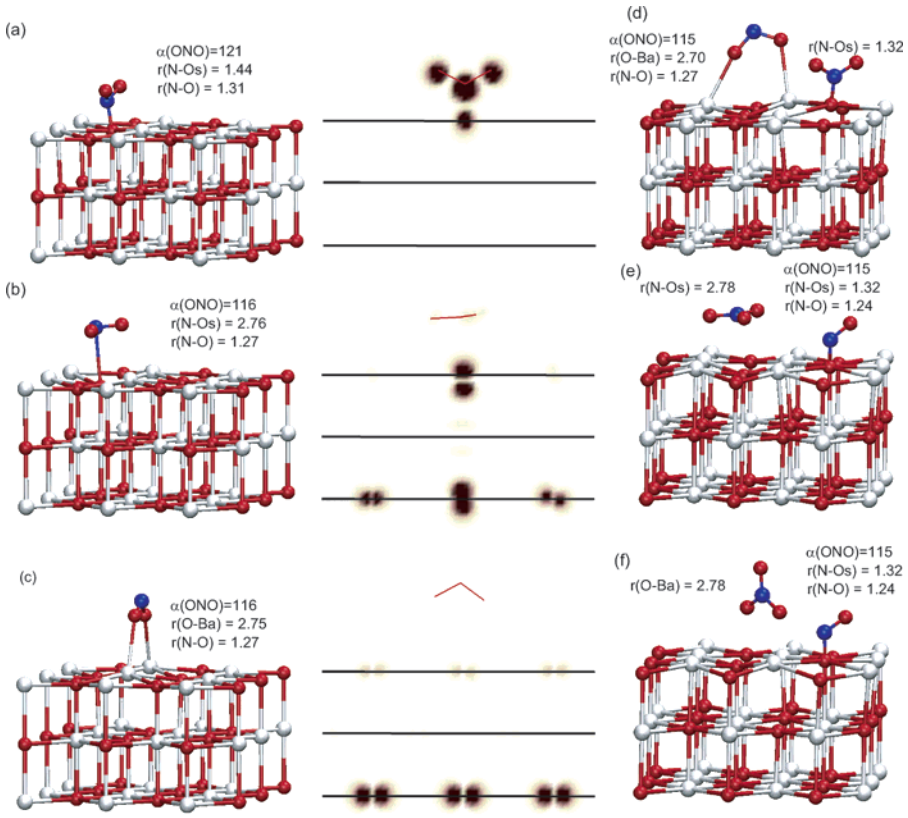

Figure 1. Optimized adsorption configurations of NO_x over BaO(100). Three structures of NO_2 are shown in (a−c), a $NO_2-Ba-O_sNO_2$ structure is shown in (d), and two NO_3-Ba-O_sNO structures are shown in (e−f). Angle is denoted by α, and the reported distances are in Å. The corresponding spin-densities are reported for (a−c). The surface layers and the NO_2 molecule are indicated by lines. The spin densities are integrated in one dimension and projected on a plane having the normal vector parallel to the surface. Color code: white (Ba), red (O), and blue (N).

similar stability, their electronic characteristics are distinctly different. For case (a), the highest occupied state is localized on the NO_3^{2-} unit, whereas for structure (b), it is delocalized over the surface anions.

The results for NO_2 adsorption are consistent with previous reports. In ref 8, case (b) was investigated at a coverage of 0.5, and an adsorption energy of 0.8 eV was reported. A structure identified as an N-down nitrite as well as (c) was studied in ref 12. Structure (c) was predicted to be the stable configuration, with an adsorption energy of 1.4 eV, whereas the adsorption energy of the N-down nitrite was reported to 0.94 eV. Also in ref 10, an N-down structure and (c) were investigated. Having an adsorption energy of 1.3 eV, structure (c) was found to be preferred over the N-down structure by 0.2 eV. The N-down structures in refs 12 and 10 are similar, having an O_s-NO_2 bond length of ∼2.2 Å and an O−N−O angle of ∼122 °. In both studies, the spin density on the adsorbate is ∼0.5 electrons. The localization of the spin density and O−N−O angle is similar to the NO_3^{2-} species in the present work. However, the present O_s-NO_2 distance is considerably shorter. In ref 11, structures (a), (b), and (c) were investigated. All configurations were calculated to have a similar (within 0.1 eV) adsorption energy of ∼1.5 eV.

Some of the quantitative energetic and structural differences with respect to previous reports can be attributed to coverage effects and/or different approximations to the exchange-correlation functional. However, qualitative differences exist, which are more likely due to differences in how the surface is modeled. All reports predict similar adsorption energy for the nitrite in the bridge configuration (c), whereas the results for the N-down nitrite (b) are in variance. A similar stability between cases (b) and (c) is calculated in slab model studies, whereas the studies using embedded clusters predict structure (b) to be less stable by ∼0.3 eV. The discrepancy is probably due to differences in allowed surface relaxation. In the present study, the contribution to the adsorption energy associated with surface relaxation is significant. For both (b) and (c), the surface distortion upon NO_2 adsorption is connected with an energy penalty of ∼0.6 eV with respect to the clean surface. The O_s anion as well as the adjacent Ba cations are, for example, explicitly involved in the relaxation following NO_2 adsorption as an N-down nitrite.

In ref 8, possible nitrite/nitrate pair structures were explored, and two were reinvestigated here. Figure 1d shows the structure of an $NO_2-Ba-O_sNO_2$ pair with the nitrite in a bridge configuration. This pair with the nitrite in the N-down structure has similar stability. As elaborated on in refs 8 and 9, the formation of nitrite-nitrate pairs, significantly increases the adsorption energy in comparison with adsorption of isolated single NO_2 radicals. The adsorption energy per NO_2 in (d) is 1.6 eV. Thus, the enhancement is 0.3 eV per NO_2. The origin of the increased stability is the pairing of electrons: one NO_2 molecule creates an electronic hole in the surface that the second molecule repairs. The $NO_2-Ba-O_sNO_2$ pair in the 0.5 coverage structure obtained in ref 8 (the nitrite in an O-down geometry over an surface cation) was not considered here. However, owing to the nondirectional character of the nitrite−surface interaction, this configuration should be of similar stability. In fact, this is supported by the simulations presented below.

A reaction between the adsorbates in Figure 1d would form NO_3-Ba-O_sNO pairs with possible structures reported in (e) and (f). For case (e), the nitrate adopts a lateral configuration, the adsorption energy per NO_2 radical is higher than for (d), being 1.8 eV per NO_2. Thus, the total energetic enhancement upon pair formation is ∼1 eV. The isomeric structure (f) with

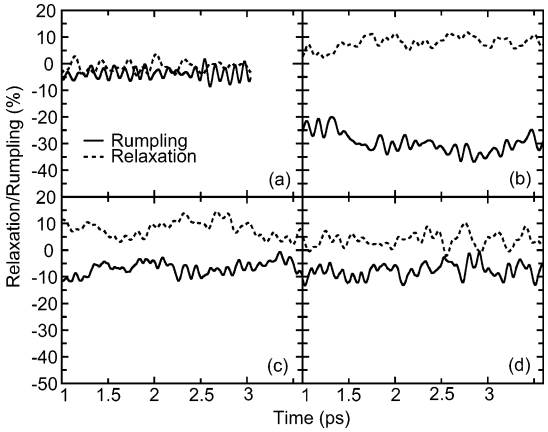

Figure 2. Relaxation and rumpling of the top BaO layer for (a) BaO(100), (b) $4NO_2$, (c) $2(NO_2-Ba-O_sNO_2)$, and (d) $2(NO_3-Ba-O_sNO)$.

the nitrate in a vertical adsorption configuration is less stable, having the adsorption energy of 1.6 eV per NO_2. Another vertical geometry with two nitrate oxygen atoms forming a Ba−Ba bridge has similar stability to case (f). The preference of the lateral structure can be rationalized by the fact that the N atom is slightly positive, as confirmed by a Mulliken population analysis. Hence, electrostatic interactions favor this configuration.

B. Dynamical Properties. Four systems were studied with respect to dynamical properties: the clean BaO(100) surface, four adsorbed nitrites, two $NO_2-Ba-O_sNO_2$ pairs, and two NO_3-Ba-O_sNO pairs. For the systems with adsorbed NO_x species, the coverage with respect to BaO units is 0.44. This is an intermediate value as the experimental saturation coverage during NO_x storage is determined to be close to unity on the basis of kinetic modeling.[7] The investigated NO_x systems are chosen, as they represent transient molecular configurations upon storage, where the final structure is proposed to be $Ba(NO_3)_2$. The temperature in the molecular dynamics simulations (300 °C) is close the operating temperature of NSR catalysts. For the clean BaO(100) surface, the optimized structure was chosen as the starting configuration. Two simulations were performed for the four NO_2 radicals, one with the nitrites initially in N-down geometries and one starting with the nitrites in bridge structures. Unless explicitly indicated, the results discussed below originate from the N-down starting configuration. For the $NO_2-Ba-O_sNO_2$ pair, the structure corresponding to a coverage of 0.5 was chosen,[8] whereas (f) in Figure 1 at proper coverage was chosen for the NO_3-Ba-O_sNO pair. The systems were evolved for ~3.6 ps (3 ps for the clean surface and 1.5 ps for the nitrite simulation, starting with bridged adsorbates), and properties were evaluated after allowing the systems to equilibrate for 1 ps.

1. BaO(100) Surface Dynamics, Effects of Adsorbates. The dynamic evolution of the BaO(100) surface was probed by calculating the relaxation and rumpling as a function of time, Figure 2. Projections of the top-layer ionic trajectories onto the *xy* plane are presented in Figure 3, and structural snapshots are reported in Figure 4.

For the clean BaO(100) surface, the average values of the relaxation and rumpling are −1.2% and −3.7%, respectively. The value for the relaxation is lower than for the zero temperature result (−3.6%), reflecting the thermal expansion of the material. The rumpling is only slightly larger than that calculated at zero temperature. Thus, the simulation indicates that it should be possible to confirm the prediction[22] of the negative sign of rumpling with measurements at room temperature. This would be of particular interest, as it, until recently, was generally believed that oxide surfaces, such as the one studied here, exhibit a positive rumpling. The maximum relaxation corresponds to 0.2 Å motions of the ions. This is in the same range as the lateral motions, Figure 3a. The maximum *xy* distance (averaged over top layer ions) from the equilibrium position is 0.2 and 0.3 Å, for the cation and anions, respectively.

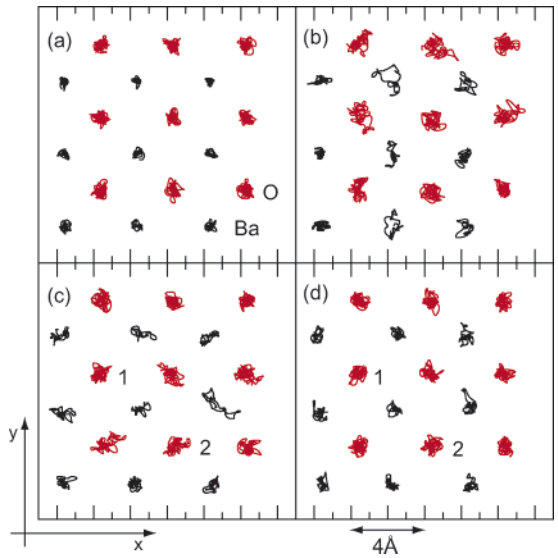

Figure 3. Projection onto the *xy* plane of the atomic trajectories in the top layer for (a) BaO(100), (b) $4NO_2$, (c) $2(NO_2-Ba-O_sNO_2)$, and (d) $2(NO_3-Ba-O_sNO)$. For clarity, the trajectories include the equilibration period. 1 and 2 in (c) and (d) correspond to O_sNO_2 and O_sNO, respectively.

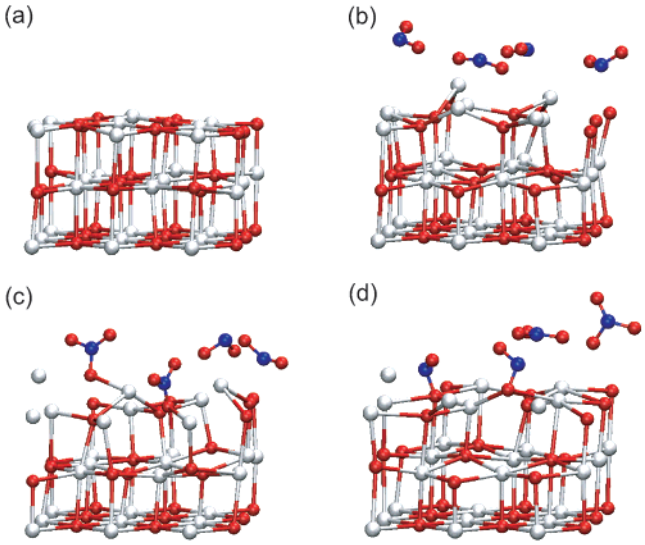

Figure 4. Snapshot taken at 2.4 ps for: (a) BaO(100), (b) $4NO_2$, (c) $2(NO_2-Ba-O_sNO_2)$, and (d) $2(NO_3-Ba-O_sNO)$. Same color code as in Figure 1.

NO_2 adsorption has a pronounced effect on the surface dynamics. The relaxation is in this case positive, with an average value of 7.9%. The rumpling is on average as large as −30% (Figure 2b). Furthermore, the adsorption has large effects on the in-plane motion of the ions, see Figure 3b. The maximum distance from the equilibrium position for the cations and anions are 0.6 and 0.5 Å, respectively. The adsorbate-induced effect of the surface dynamics is owing to the adsorbate−surface bond mechanism, which includes charge transfer from the surface to the NO_2 radicals, forming nitrites. Analyzing the charge density at various stages along the simulations reveals that close to four

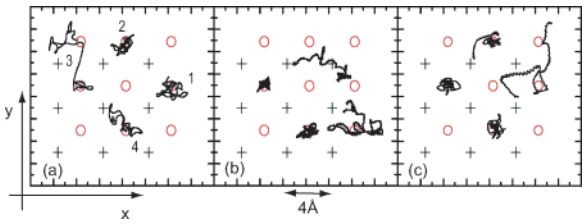

Figure 5. Projections of the N atom trajectories onto the *xy* plane for (a) $4NO_2$, (b) $2(NO_2-Ba-O_sNO_2)$, and (c) $2(NO_3-Ba-O_sNO)$. Crosses and rings represent the optimized positions for the top-layer Ba and O ions, respectively. For clarity the trajectories include the equilibration period.

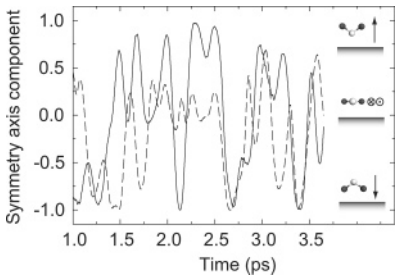

Figure 6. Time evolution of the *z* component of the symmetry unit axis of nitrite 1 (solid line) and 2 (dashed line) in the simulation of $4NO_2$. The molecular orientations corresponding to 1, 0, and −1 are schematically indicated.

electrons have been transferred from the surface to the adsorbates. This is consistent with the spin-density analysis in the static calculation. The formation of nitrites is also supported by structural signatures. For all adsorbates, the O−N−O angle is oscillating around ∼117°. Because the electrons are transferred from delocalized O(2p) states, the surface has delocalized electron holes that destabilize the surface. The reduced screening between cations is one contribution to the positive relaxation and pronounced rumpling. A second contribution is the electrostatic interaction between the adsorbates and the surface ions. The anions are pushed into the surface, whereas the cations move to coordinate toward the adsorbates. The snapshot in Figure 4b illustrates such an event.

In Figure 2, parts c and d, the relaxation and rumpling are reported for the two pair configurations. As in the case of NO_2 adsorption, the relaxations are positive, and the average values are 8.0 and 3.8% for (c) and (d), respectively. The positive relaxation is of the same origin as discussed for NO_2 adsorption. For both $NO_2-Ba-O_sNO_2$ and NO_3-Ba-O_sNO, the rumpling is larger than that for the clean surface. However, it is not as large as in the case of the four nitrites. The average values are −6.7 and −7.7% for (c) and (d), respectively. The decreased rumpling upon pair formation is owing to the electron stabilization in the surface layer. The cation dynamics in the *xy* plane is similar for the four nitrites and the two $NO_2-Ba-O_sNO_2$ pairs (Figure 3c). This could be attributed to the interaction with the mobile nitrites, discussed in detail in the next section. For the NO_3-Ba-O_sNO system (Figure 3d), the projected cation motion is comparable with the result for the clean surface.

2. NO_x Adsorbate Dynamics. The projections of the N-atom trajectories onto the *xy* plane in the three systems of adsorbed NO_x species are reported in Figure 5. As already mentioned, the interaction between the adsorbed NO_2 radicals (forming nitrites) and the surface is of an electrostatic nature and only weakly directional. This has a large effect on the dynamics of the nitrites, which is shown in Figure 5a. For three of the nitrites, the motion during the simulation is close to the initial oxygen site. In contrast, for molecule 3, a diffusion event is observed, where the nitrite diffuses between two oxygen sites. The transition structure is a Ba−ONO configuration, with a Ba−ONO distance of 2.7 Å. However, because of the high flexibility of the nitrites, the transition structure is probably not unique.

The average distance between the oxygen atoms in the surface and the nitrogen atoms in the nitrites is 3.1 Å. This is slightly larger than the N-down nitrite distance in Figure 1b. The nitrite motion in the *z* direction is significant, spanning ∼2 Å. The bridging configuration discussed in connection with the static calculation is not populated for any of the nitrites, although the O atoms of the nitrites occasionally coordinate toward the surface cations. The bridge configuration is avoided for entropy reasons. The same holds for the NO_3^{2-} structure, which, moreover, would require a localization of charge. Thus, this configuration could be difficult to access by performing the simulation in an electronic singlet state.

In addition to the *xy* dynamics, the nitrites possess rotational motions. In fact, the simulations reveal a continuous interconversion between different molecular orientations. This is clearly shown in Figure 6 where the *z* component (normal to the surface) of the symmetry unit axis of the nitrites are reported. Because the qualitative time evolution of the symmetry axis is similar for all nitrites, for clarity, only the results for 1 and 2 in Figure 5a are included. A rotational event of nitrite 1 (solid line) is, for example, observed between 2.0 and 2.25 ps in the graph.

To investigate if the initial configuration influences the general results of the nitrite dynamics, a shorter simulation was performed, starting with the nitrites in bridge structures. This simulation confirmed the results of the longer simulation that the Ba−ONO−Ba bridge configuration is avoided at elevated temperatures. All four nitrites immediately moved away from their bridge sites and, within ∼0.5 ps, occupied a distribution of different orientations over surface anions.

For the $NO_2-Ba-O_sNO_2$ configuration, Figure 5b, the motions of the nitrates are restricted in the *xy* plane. Vertically, however, these species move within a range of 1.4 Å. For this system, the dynamics of the nitrites are similar to the one discussed for the system of adsorbed NO_2 radicals. The starting configuration of this system was chosen, with the nitrites in the position predicted from calculations at 0.5 coverage.[8] The nitrite was in this case positioned over a cation. In the simulation, however, the nitrites immediately leave these positions to occupy structures over the surface anions. This is consistent with the results of the simulation of the four nitrites.

The motion of the nitrites are restricted for the NO_3-Ba-O_sNO configuration, Figure 5c. However, in similarity with the nitrates for $NO_2-Ba-O_sNO_2$, the nitrite motion normal to the surface is considerable, spanning 1.5 Å. The starting configuration in this simulation has the nitrates in vertical positions (Figure 1f). However, as suggested from the static calculations, this corresponded to an unfavored configuration. In the beginning of the simulation, the nitrates convert to lateral configurations. Still, the vertical configuration appeared to be relevant for the two diffusion events observed for one of the nitrates, see Figure 5c. During the diffusion, the nitrate tumbles between oxygen sites while occupying vertical structures. In the first event, the transition structure is bidentate, with two nitrate oxygens coordinating toward one Ba cation. The $Ba-O_2NO$ distances are ∼2.8 Å. In the second event, the transition structure is monodentate, with a $Ba-ONO_2$ distance of 2.7 Å. Although both diffusion events include tumbling, the exact vertical configuration (mono- or bidentate) does not seem to be crucial.

The geometry-optimized $NO_2-Ba-O_sNO_2$ and NO_3-Ba-O_sNO pairs display similar stabilities, with a slight preference

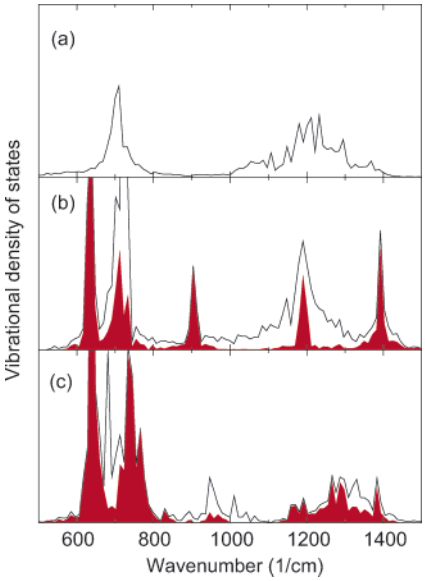

Figure 7. Vibrational density of states (VDOS) for (a) $4NO_2$, (b) $2(NO_2-Ba-O_sNO_2)$, and (c) $2(NO_3-Ba-O_sNO)$. In (b) and (c), the VDOS corresponding to the nitrates has been shaded.

for NO_3-Ba-O_sNO. It is interesting to study if this situation remains at the temperature considered in the simulation. Analyzing the adsorption energy per NO_2 along the simulation shows that this is the case. On average, the NO_3-Ba-O_sNO pair is preferred by 0.2 eV per NO_2, although situations may occur where the reverse applies. If the used surface model had allowed for larger lateral motion (larger simulation cell), we anticipate situations where surface nitrates and adsorbed nitrates would interconvert.

C. Vibrational Analysis. Infrared spectroscopy is a common technique for in situ characterization of surface species. The interpretation of experimental vibrational spectra is, however, often ambiguous due to many possible adsorption configurations and overlapping bands from different adsorbates. In a previous study, the same computational technique was used, with a cluster description of BaO, to study the vibrational properties of NO_x adsorbed on BaO.[9] In ref 9, the vibrational frequencies were calculated for some adsorption configurations using the method of finite differences. Here, the atomic trajectories are used to evaluate the vibrational spectra. The results for the three different systems of nitrites and nitrates are reported in Figure 7.

For the system of adsorbed NO_2 radicals, two main vibrational features exist, centered at 700 cm^{-1} and 1200 cm^{-1}, respectively. The 700 cm^{-1} band corresponds to O−N−O bending modes, whereas the broad 1200 cm^{-1} feature corresponds to different N−O stretch vibrations. For the gas-phase nitrite, the vibrational wavenumbers are calculated to 720, 1277, and 1243 cm^{-1}, for the bending, asymmetric, and symmetric stretch vibration, respectively. In ref 9, the wavenumbers calculated for NO_2 adsorbed as a nitrite in the N-down configuration were 770, 1299, and 1304 cm^{-1} for the O−N−O bending, the asymmetric, and symmetric N−O stretch vibration, respectively. The corresponding modes for the bridging nitrite structure were evaluated to be 755, 1228, and 1290 cm^{-1}, respectively.[9]

The origin of the broad feature centered at 1200 cm^{-1} is revealed by analyzing the vibrational modes for each of the nitrites. The result of such a decomposition is presented in Figure 8, where the same nitrite numbering as in Figure 5 is used. In the simulation, molecules 3 and 4 experience a higher mobility than 1 and 2. The broadening in the vibration spectra clearly correlates with the motion of the nitrite in the *xy* plane.

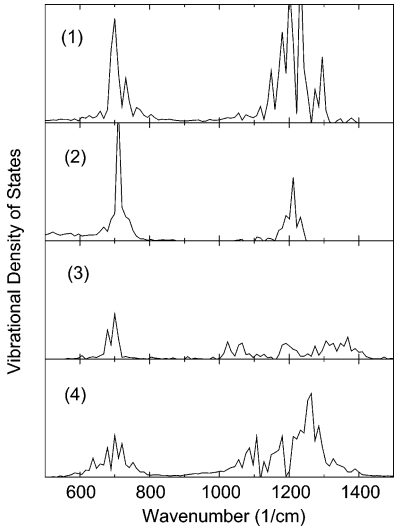

Figure 8. Vibrational density of states for the four NO_2 molecules. The same numbering as in Figure 5 applies.

Experiments based on infrared spectroscopy have shown that NO_2 adsorption over BaO at 300 °C leads to nitrate formation.[9] During the course of the simulation, spontaneous nitrate formation is not observed. The reason for the difference is presumably the high density of vacancies, steps, and corner sites in the experiments, as well as the short simulation time when comparing to experimental time scales. In ref 9, the adsorption temperature was decreased to 30 °C to prevent nitrate formation. At this temperature, a broad high-intensity peak centered at 1330 cm^{-1} appeared, together with a broad peak with lower intensity at 1250 cm^{-1}. These measurements are consistent with the results from the simulations with the broad structured feature between 1150 and 1350 cm^{-1} in Figure 7a.

For the $NO_2-Ba-O_sNO_2$ pairs, Figure 7b, there is a clear difference between the O_sNO_2 species and the mobile nitrites. For the anchored species, the peaks are narrow, with distinct features at 900, 1200, and 1400 cm^{-1} for N−O stretching modes. The bending modes appear at lower frequencies. For the gas-phase nitrate, the calculated vibrational modes are: scissors mode at 623 cm^{-1} (2-fold degenerated), umbrella mode at 795 cm^{-1}, symmetric stretch at 1005 cm^{-1}, and asymmetric stretch at 1344 cm^{-1} (2-fold degenerated). Anchoring the nitrate lowers the symmetry from D_{3h} to C_{2v}, which lifts the degeneracy of the asymmetric stretch vibrations. The modes corresponding to the nitrites are spread over a wide interval, with features resembling the results of the four nitrites. In ref 9, the wavenumbers for the N−O stretch vibrations of a similar nitrate species were calculated to 999, 1291, and 1448 cm^{-1}, respectively.

In the case of the NO_3-Ba-O_sNO pairs, the nitrites are anchored to the surface, whereas the nitrates are mobile. For the nitrites, features corresponding to $N-O_s$ stretch vibrations appear at ∼950 cm^{-1}. These are not present for the mobile nitrites in Figure 7, parts a and b, and consequently, are an exclusive signature of this type of nitrites. The bending modes at 700 cm^{-1} are not shifted with respect to the mobile nitrites. In ref 9, the N−O stretch modes for nitrite in the anchored configuration were reported at 1397 and 1140 cm^{-1}, respectively. In the case of the nitrates, both vertical and lateral structures are occupied. For the vertical structure, the spectrum resembles that of the nitrate in Figure 7b. However, the peak in the vibrational density of states corresponding to the symmetric stretching at 900 cm^{-1} has decreased. For the lateral structure, the two asymmetric N−O stretch vibrations are nearly

degenerated, with one feature just below 1300 cm^{-1}. This is consistent with the spectrum for the gas-phase nitrate.

IV. Conclusions

Ab initio molecular dynamics simulations have been used to explore adsorbed NO_x species on the BaO(100) surface. The simulations reveal and clarify several aspects of the interaction between BaO and NO_x. Nitrites and nitrates are found to be mobile, with spontaneous diffusion events appearing on the short time scale of the simulations. The interaction between nitrites and the surface is of electrostatic character. At elevated temperatures, adsorbed nitrites continuously adopt new configurations. However, these configurations are predominantly restricted to such, with the nitrites located over surface anions. Although similar in stability, the Ba−ONO−Ba bridging configuration is avoided during the course of the simulations. For nitrates, the preferred orientation during the simulations is a lateral structure with the N atom over a surface anion. Nitrate diffusion between anion sites was found to occur via a tumbling motion, involving a molecular configuration with nitrate oxygen atoms coordinated toward surface Ba cations.

The dynamical response of the BaO(100) surface is found to strongly depend on the nature of the surface−adsorbate interaction. Nitrite formation implies electron abstraction from the surface. This results in a significantly more flexible surface than for the clean surface or the case with nitrite-nitrate pairs. The mean rumpling of the oxidized surface is as large as −30%, which should be compared to −4% for the clean surface or −7% for the pairs.

The continuous interconversion between different adsorption structures for nitrites is reflected in broad vibrational signatures. This explains infrared spectroscopy measurements of adsorbed nitrites on BaO.[9] The prediction of high mobility of NO_x species at elevated temperatures justifies the use of spillover mechanism in microkinetic models of the NO_x storage mechanism[7] from first principles.

Acknowledgment. The authors thank Erik Fridell and Magnus Skoglundh for valuable discussions. CPU time granted at the Center for Parallel Computers and National Supercomputer Centre in Sweden is gratefully acknowledged. The Competence Centre for Catalysis is hosted by Chalmers University of Technology and financially supported by the Swedish Energy Agency and the member companies AB Volvo, SAAB Automobile Powertrain AB, Johnson Matthey CSD, Perstorp AB, Albemarle Catalysts, AVL-MTC AB, and the Swedish Space Corporation.

References and Notes

(1) *Handbook of Catalysis*; Ertl, G., Knözinger, H., Weitkamp, J., Eds.; Wiley-VCH: Weinheim, 1997.

(2) Grönbeck, H. *Top. Catal.* **2004**, *28*, 59.

(3) Bögner, W.; Krämer, M.; Krutzcsh, B.; Pischinger, S.; Voigtländer, D.; Wenninger, G.; Wirbeleit, F.; Brogan, M.; Brisley, R. J.; Webster, D. E. *Appl. Catal., B* **1995**, *7*, 153.

(4) Takahashi, N.; Shinjoh, H.; Iijima, T.; Suzuki, T.; Yamazaki, K.; Yokota, K.; Suzuki, N.; Miyoshi, N.; Matsumoto, S.; Tanizawa, T.; Tanaka, T.; Kasahara, K. *Catal. Today* **1996**, *27*, 63.

(5) Takeuchi, M.; Matsomoto, S. *Top. Catal.* **2004**, *28*, 151.

(6) Fridell, E.; Persson, H.; Westerberg, B.; Olsson, L.; Skoglundh, M. *Catal. Lett.* **2000**, *66*, 71.

(7) Olsson, L.; Persson, H.; Fridell, E.; Skoglundh, M.; Andersson, B. *J. Phys. Chem. B* **2001**, *105*, 6895.

(8) Broqvist, P.; Panas, I.; Fridell, E.; Persson, H. *J. Phys. Chem. B* **2002**, *106*, 137.

(9) Broqvist, P.; Grönbeck, H.; Fridell, E.; Panas, I. *J. Phys. Chem. B* **2004**, *108*, 3523.

(10) Karlsen, E. J.; Nygren, M. A.; Petterson, L. G. M. *J. Phys. Chem. B* **2003**, *107*, 7795.

(11) Schneider, W. F. *J. Phys. Chem. B* **2004**, *108*, 273.

(12) Branda, M. M.; Valentin, C. D.; Pacchioni, G. *J. Phys. Chem. B* **2004**, *108*, 4752.

(13) Schneider, W. F.; Hass, K. C.; Miletic, M.; Gland, J. L. *J. Phys. Chem. B* **2002**, *106*, 7405.

(14) Prinetto, F.; Ghiotti, G.; Nova, I.; Lietti, L.; Tronconi, E.; Forzatti, P. *J. Phys. Chem. B* **2001**, *105*, 12732.

(15) Odelius, M. *Phys. Rev. Lett.* **1999**, *82*, 3919.

(16) Giordano, L.; Goniakowski, J.; Suzanne, J. *Phys. Rev. B* **2000**, *62*, 15406.

(17) Langel, W. *Chem. Phys. Lett.* **1996**, *259*, 7.

(18) Car, R.; Parrinello, M. *Phys. Rev. Lett.* **1985**, *55*, 2471.

(19) Andreoni, W.; Curioni, A. *Parallel Comput.* **2000**, *26*, 819.

(20) Marx, D.; Hutter, J. *Modern Methods and Algorithms in Quantum Chemistry*; Forschungzentrum Juelich NIC Series; Forschungzentrum Juelich GmbH: Juelich, 2000; Vol. 1.

(21) *CPMD*, version 3.9.1; Copyright IBM Corp., 1990−2001; Copyright MPI fuer Festkoerperforschung: Stuttgart, 1997−2001.

(22) Broqvist, P.; Grönbeck, H.; Panas, I. *Surf. Sci.* **2004**, *554*, 262.

(23) Grönbeck, H.; Broqvist, P. *J. Chem. Phys.* **2003**, *119*, 3896.

(24) Perdew, J.; Burke, K.; Ernzerhof, M. *Phys. Rev. Lett.* **1996**, *77*, 3865.

(25) Troullier, N.; Martins, J. L. *Phys. Rev. B* **1991**, *43*, 1993.

(26) Wertheim, G. K. *J. Electron. Spectosc. Relat. Phenom.* **1984**, *34*, 309.

(27) Increasing the cutoff to 80 Ry did not change the adsorption energy and structure of the NO_3^{2-} configuration within 0.01 eV and 0.01 Å, respectively.

(28) Effects of the vacuum width was tested for the stable nitrite/nitrate pair configuration. Increasing the vacuum width to 15 Å did not change the adsorption energy and structure within 0.01 eV and 0.01 Å, respectively.

(29) Barnett, R. N.; Landman, U. *Phys. Rev. B* **1993**, *48*, 2081.

(30) Chang, Z. P.; Graham, E. K. *J. Phys. Chem. Solids* **1977**, *38*, 1355.

(31) Königstein, M.; Catlow, C. R. A. *J. Solid State Chem.* **1998**, *140*, 103.

(32) Lide, D. R., Ed. *Handbook of Chemistry and Physics*, 71st ed.; CRC Press: Boca Raton, FL, 1990−1991.

(33) A bidentate nitrite structure bonded to a surface cation was found to be 0.3 eV less stable than the nitrite in the "N-down" configuration. Coordinating the NO_2 via the nitrogen atom to the cation did not correspond to a minimum.